Available on CMS information server

CMS CR -2016/200

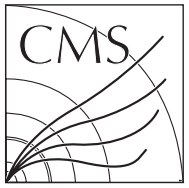

The Compact Muon Solenoid Experiment

Conference Report

Mailing address: CMS CERN, CH-1211 GENEVA 23, Switzerland

27 August 2016 (v2, 28 August 2016)

The X(750000) and the latest Higgs results from the CMS Detector of the LHC

Maria Isabel Pedraza Morales for the CMS Collaboration

Abstract

Despite the discovery of the Higgs boson, which contributed to the success of the Standard Model, there are at least 60 different analyzes carried out in parallel with the CMS detector looking for new physics. In particular the small excess seen about 750 GeV by the two general purpose experiments at the LHC, CMS and ATLAS, that can not be explained by the particles of the standard model. In this talk the current status of the Higgs analysis and the search for physics beyond the Standard Model in the two photons final state is presented.

Presented at *DPC-SMF2016 XXX Reunion Anual de la Division de Particulas y Campos de la SMF*

The diphoton resonance and Higgs results from the CMS Detector of the LHC

M.I.Pedraza-Morales on behalf of the CMS Collaboration

Facultad de Ciencias Físico-Matemáticas, Benemérita Universidad Autónoma de Puebla

E-mail: mpedraza@fcfm.buap.mx

Abstract. Despite the discovery of the Higgs boson, which contributed to the success of the Standard Model, there are at least 60 different analyzes carried out in parallel with the CMS detector looking for new physics. In this talk the current status of the Higgs analysis and the search for physics beyond the Standard Model in the two photons final state are presented.

1. Introduction

During the Run I of the CERN LHC, a new particle was discovered by both ATLAS [4] and CMS [5] collaborations. Subsequent studies using the full LHC Run I data set in various decay channels and production modes and combined measurements from ATLAS and CMS [[6]-[18]] showed that the properties are so far consistent with expectations from the Standard Model Higgs boson.

In this paper, the results with the Run II of the most sensitive channels with a mass around 125 GeV are $H \to ZZ \to 4l$ and $H \to \gamma\gamma$ are presented, including the search for resonant production of high mass photon pairs. The analyses followed the strategy described in [9], [10] and [11] respectively. The data collected by CMS in 2016 so far corresponds to 12.9 fb^{-1} of integrated luminosity of pp collisions at $\sqrt{s} = 13\ TeV$.

2. CMS Detector

The Compact Muon Solenoid (CMS) [12] is a multipurpose detector operating at the Large Hadron Collider (LHC) at CERN, which has been successfully collecting data since 2009. The central feature is a superconducting solenoid, 13m in length and 6m in diameter, which provides an axial magnetic field of 3.8 T. CMS detector subsystems relevant for these searches are the tracker (silicon pixel and strip tracker), the electromagnetic calorimeter (ECAL), the hadronic calorimeter, and the muon spectrometer. The physical objects used in these analyses are built as follows: Muons are reconstructed independently in the tracker and the muon spectrometer, and are combined using statistical combination; electrons are reconstructed from clusters of ECAL cells with a matched track in the tracker; and photons is directly obtained from the ECAL measurement. A particle-flow event algorithm [[13], [13]] reconstructs and identifies each individual particle with an optimised combination of information from the various elements of the CMS detector.

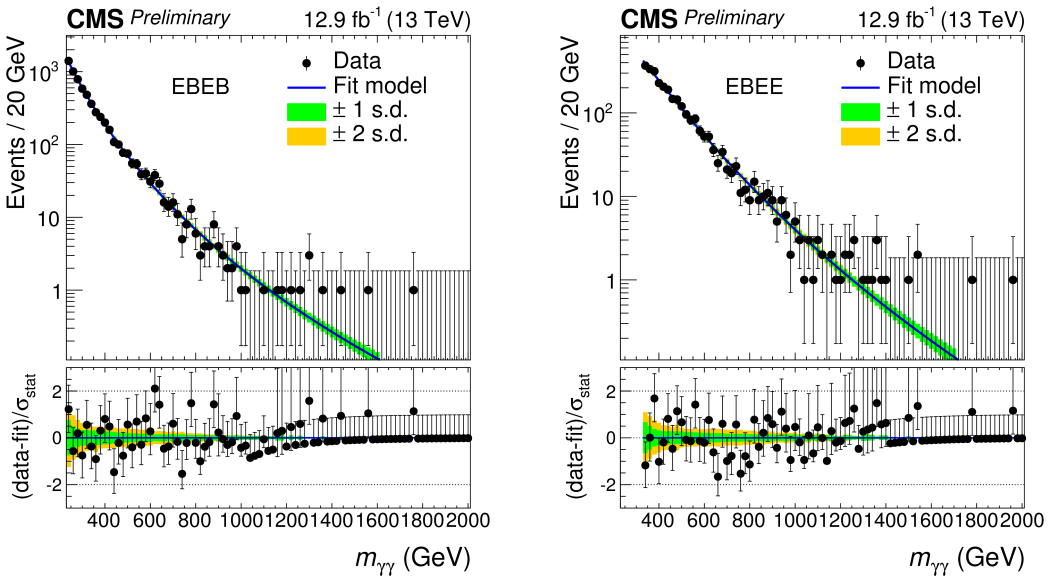

Figure 1. Observed invariant mass spectra for the EBEB (Left) and EBEE (Right). No event with $m_{\gamma\gamma} > 2000$ GeV is selected in the analysis. The results of a likelihood fit to the background-only hypothesis are also shown. The shaded regions show the 1 and 2 standard deviation uncertainty bands associated with the fit, and reflect the statistical uncertainty of the data. The lower panels show the difference between the data and fit, divided by the statistical uncertainty in the data points.

3. Data Sets

These analyses makes use of an integrated luminosity of 12.9 fb^{-1} of pp collisions collected by the CMS experiment at $\sqrt{s} = 13$ TeV in 2016. The main triggers for the $H \to ZZ \to 4l$ analysis select either a pair of electrons or muons, or an electron and a muon. While a diphoton trigger with asymmetric transverse energy (ET) thresholds are used for the $H \to \gamma\gamma$ analysis, and the high mass photon pairs search. The trigger selection is fully efficient for resonance masses above 500 GeV.

All signal and background generators are interfaced with PYTHIA 8 [15] to simulate the multiparton interaction and hadronization effects. The generated events go through a detailed simulation of the CMS detector based on GEANT4 [16] and are reconstructed with the same algorithms that are used for data. The simulated events include pp interactions and have been reweighted so that the distribution of the number of interactions per LHC bunch crossing matches that observed in data.

4. Diphoton resonances

The diphoton channel provides fully reconstructed resonances with a good mass resolution, an opportunity to discover new particles. It is an experimentally robust channel with small systematic uncertainties and relatively low background at hadron colliders. The event selection looks for final states with two high-p_T isolated photons passing the selection of $p_T > 75$ GeV, $|\eta| < 2.5$, excluding the transition barrel-encap region $1.44 < |\eta| < 1.57$. Two event categories are defined EBEB (both γ's in the barrel), and EBEE(only one γ in the barrel, one in the endcap). The background model is a parametric fit to data with an empirical function $f(m_{(\gamma\gamma)}) = m_{\gamma\gamma}^{a+b*log(m_{\gamma\gamma})}$. The mass spectra is shown in Figure 2 for both categories.

The signal shape is a convolution of intrinsic line-shape of the resonance, derived using

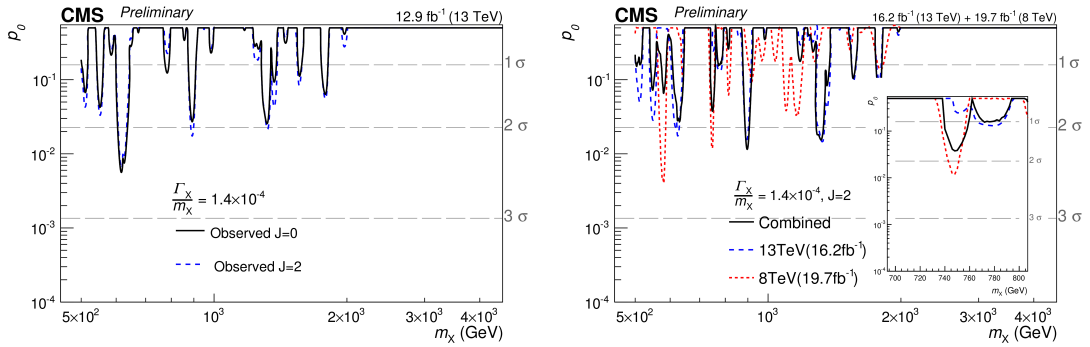

Figure 2. (Left) Observed background-only p-value for resonances with $\Gamma_X/m_X = 1.4\times10^{-4}$ as a function of the resonance mass m_X, from the analysis of the 12.9 fb^{-1} data collected at $\sqrt{s} = 13$ TeV in 2016. (Left) Observed background-only p-value for resonances with $\Gamma_X/m_X = 1.4\times10^{-4}$ and spin-2 as a function of the resonance mass m_X, from the combined analysis of the 8 and 13 TeV data [1].

PYTHIA, and detector resolution. The signal mass resolution, quantified through the ratio of the full width at half maximum of the distribution, divided by 2.35, to the peak position, is roughly 1% and 1.5% for the EBEB and EBEE categories respectively. Nine mass values in the range 500-4500 GeV with spin-0 and spin-2 with the value of the width $\Gamma_X/m_X = 1.4\times10^{-4}$, 1.4×10^{-2}, 5.6×10^{-2} were tested. The observed p-value obtained for selected width is shown in Figure 2. No significant excess in proximity of 750 GeV.

5. Higgs boson studies

5.1. Diphoton

The event selection requires two photon candidates with $p_T^1 > 30$ and $p_T^2 > 20$. Both photons must satisfy the requirement $|\eta| < 2.5$, excluding the transition region between the barrel and the endcap $1.44 < |\eta| < 1.57$. Aditionally the energy sum of 3X3 crystals centered on the most energetic crystal in the candidate electromagneticmagnetic cluster divided by the energy of the candidate (R_9 variable) should be larger than 0.8, or the charged hadron isolation $< 20\ GeV$, or the charged hadron isolation relative to $p_T < 0.3$.

In order to increase the signal background ratio and improve the analysis sentivity the events are divided into eight categories, labelled as: ttH Leptonic Tag, ttH Hadronic Tag, VBF Tag 0, VBF Tag 1, Untagged 0, Untagged 1, Untagged 2 and Untagged 3. Figure 3 shows the multivariate discriminator used to define the Untagged categories, labelled from best resolution to worst (left) and the shows the invariant mass for all categories (right). The dominant background to $H\to\gamma\gamma$ consists of the irreducible prompt diphoton production, and the reducible backgrounds from $\gamma+jet$ and QCD multijet, where the jets are misidentified as isolated photons. The model used to describe the background is extracted from data with the discrete profiling method [17].

A significance of 5.6 σ is observed (6.2 σ expected) at 125.09 GeV. The best fit for the signal is strength $\hat{\mu} = \sigma/sigma_{SM} = 0.95^{+0.21}_{-0.18} = 0.95 \pm 0.17(stat.)^{+0.08}_{-0.05}(theo.)^{+0.10}_{-0.07}(syst.)$. The signal strength is also measured for the bosonic and fermioninc components $\hat{\mu}_{VBF,VH} = 1.59^{+0.73}_{-0.45}$ and $\hat{\mu}_{ggH,t\bar{t}H} = 0.8^{+0.14}_{-0.18}$. Figure 4 shows the signal strength per production processes. The production mechanism signal strengths are compatible with the SM.

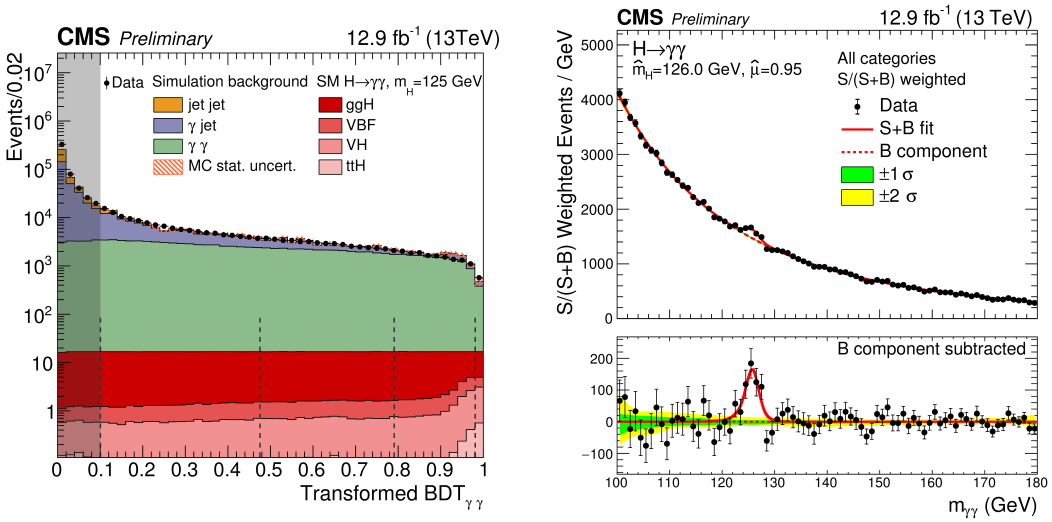

Figure 3. (Left) Transformed $BDT_{\gamma\gamma}$ classifier score in data (black points) and simulation (stacked histograms) for events in the region $100 < m_{\gamma\gamma} < 180\ GeV$. Dashed vertical lines separate the Untagged categories from left (Untagged 0) to right (Untagged 3). The gray band represents events rejected in the analysis. (Right) Data points (black) and signal plus background model fits for all categories summed weighted by their sensitivity. The 1 standard deviation (green) and 2 standard deviation bands (yellow) include the uncertainties of the fit. The bottom plot shows the residuals after background subtraction.

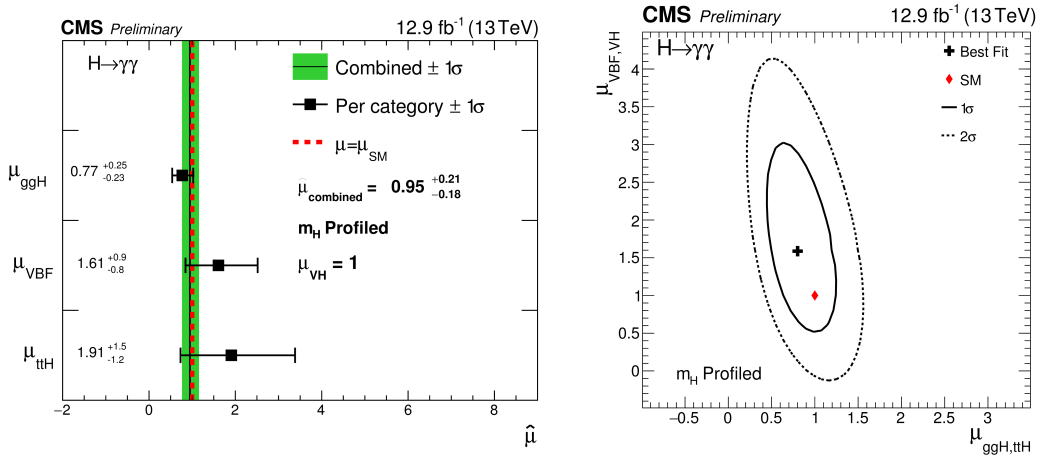

Figure 4. (Left) Signal strength measured for each process (black points) for profiled m_H, compared to the overall signal strength (green band) and to the SM expectation (dashed red line). Since this analysis does include any categories targeting the VH process, we impose $\mu_{VH} = 1$. (Right) The two-dimensional best-fit (black cross) of the signal strengths for fermionic (ggH, $t\bar{t}H$) and bosonic (VBF, ZH, WH) production modes compared to the SM expectations (red diamond). The Higgs boson mass is profiled in the fit. The solid (dashed) line represents the 1 standard deviation (2 standard deviation) confidence region.

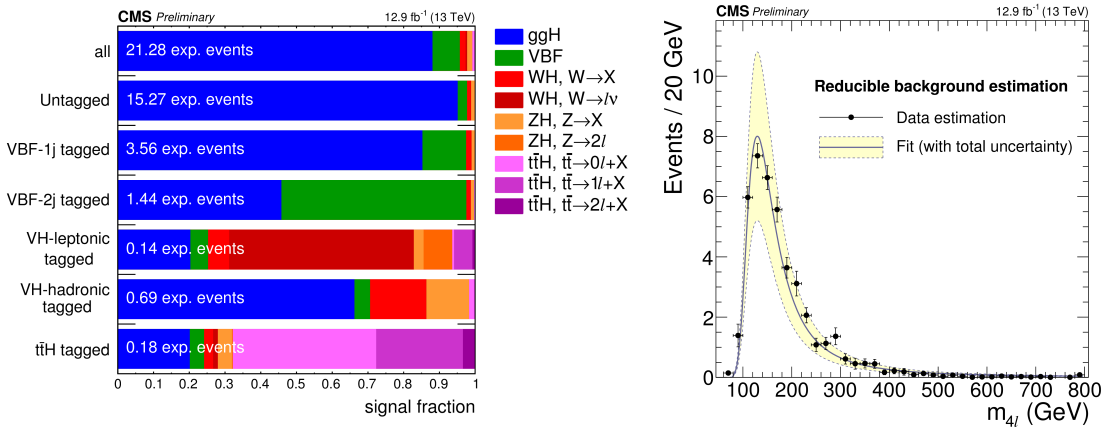

Figure 5. (Left) Signal relative purity of the six event categories in terms of the 5 main production mechanisms of the H(125) boson in a $118 < m_{4l} < 130$ GeV window. The WH, ZH and $t\bar{t}H$ processes are split according to the decay of associated objects, whereby X denotes anything else than a lepton. (Right) Combination of the OS and SS method predictions for the reducible background in the signal region and the parametrized m_{4l} shape. The yellow band shows the total uncertainty on the prediction.

5.2. Four leptons

This analysis relies on the efficiency to select leptons, the large signal background ratio, excellent resolution, and the complete reconstruction of the final state. It is called *the golden channel* for discovery and property measurements. The event selection requires at least 4 leptons in the event, Z candidates are then built with pairs of leptons of the same flavor and opposite-charge (e^+e^-, $\mu^+\mu^-$) and required to have $12 < m_{l^+l^-} < 120$ GeV. Then they are combined into ZZ candidates, we denote as Z_1 the Z candidate with an invariant mass closest to the nominal Z boson mass. The flavors involved define three subchannels: $4e$, 4μ and $2e2\mu$.

The events are separated in 6 mutually exclusive categories in order to increase sensitivity, relying on the number of jets, b-tags, additional leptons, and cuts on the 4 production discrminants. The Figure 5 shows the signal fraction for each category. The main and irreducible background is the ZZ production, the reducible background comming from $Z+X$ is data driven estimated. Two independent methods are applied : Same-sign (SS) and Opposite-sign (OS), using orthogonal control regions. The Figure 5 shows the reducible background estimation using both methods.

The results of the event selection shows a good agreement over the whole range of m_{4l} in the three final states ($4e$, 4μ and $2e2\mu$). The highest-mass candidate has a mas of 802 GeV. Figure 6 shows the invariant mass combined. The observed significance from simultaneous fit of the 2D lieklihood in 3 final states by 6 categories is 6.2 σ (6.5σ expected) at $125.09GeV$, the mass value obtained in the combination of Run1 [18]. Figure 6 shows the minimum of p-value gotten at $m_H = 124.3$ GeV, a significance of 6.4 σ is observed (6.3 σ expected).

The combined signal strength at $m = 125.09$ is $\hat{\mu} = 0.99^{+0.33}_{-0.26}$. The signal strength is also measured for the bosonic and fermioninc components $\hat{\mu}_{VBF,VH} = 0.91^{+1.56}_{-0.91}$ and $\hat{\mu}_{ggH,t\bar{t}H} = 1^{+0.39}_{-0.32}$. Figure 7 shows the signal strength per production processes. The production mechanism signal strengths are compatible with the SM.

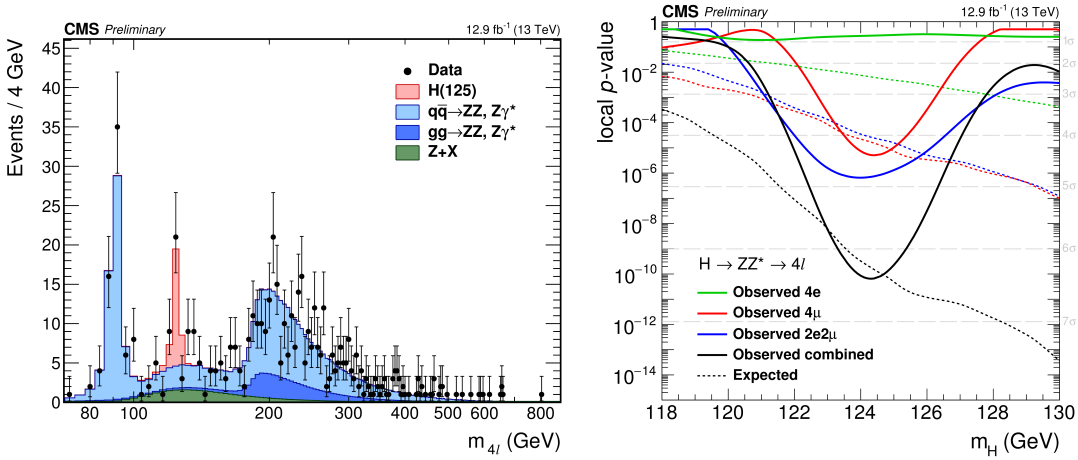

Figure 6. (Left) Distribution of the four-lepton reconstructed invariant mass m_{4l} in the full mass range. Points with error bars represent the data and the stacked histograms represent expected distributions from the 125 GeV Higgs boson signal and the ZZ backgrounds, both normalized to the SM expectation. (Right) Significance of the local fluctuation with respect to the SM expectation as a function of the Higgs boson mass. Dashed lines show the mean expected significance of the SM Higgs boson for a given mass hypothesis

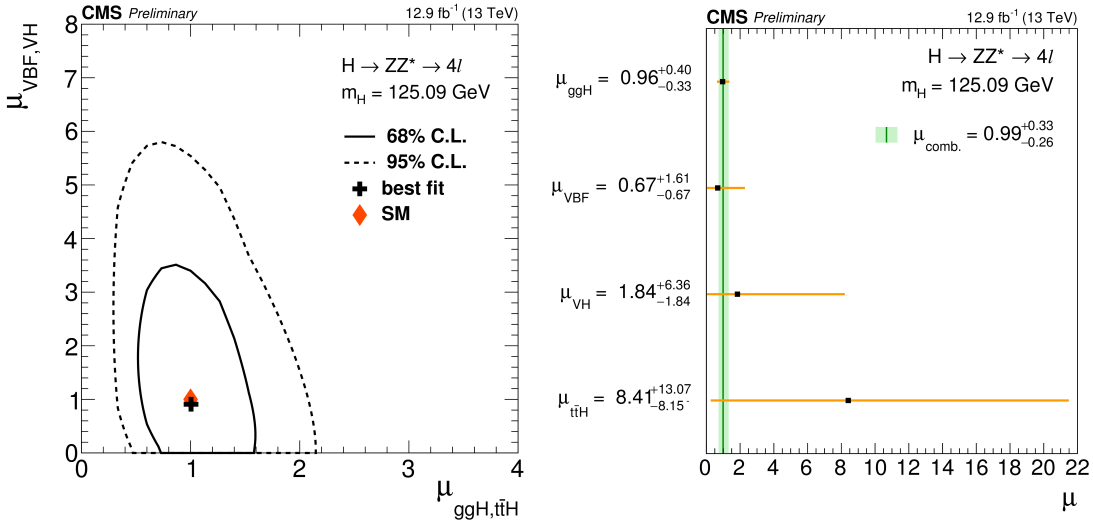

Figure 7. (Left) Result of the 2D likelihood scan for the $\mu_{ggH,t\bar{t}H}$ and $\mu_{VBF,VH}$ signal strength. The solid and dashed contours show the 68% and 95% CL regions, respectively.The cross indicates the best-fit values, and the diamond represents the expected values for the SM Higgs boson. (Right) Results of likelihood scans for the signal strength corresponding to 4 main Higgs boson production modes, compared to the combined μ shown as a vertical line. The horizontal bars and the filled band indicate the $\pm 1\sigma$ uncertainties. The uncertainties include both statistical and systematic sources.

Summary
The observation of the Higgs boson decaying in the four lepton and the diphoton channel and the measurement of some of its properties is presented, as well as the search for diphoton resonances in the high mass region. The analysis used 12.9 fb^{-1} of data collected by the CMS experiment in 2016. The analyses follow closely the strategies used for Run 1. A clear signal, of the Higgs boson in both channels, is observed. The observed significance at $m_H = 125.09$ in the four lepton channel is 6.2 σ, and in the diphoton channel is 5.6 σ. No significant excess of events was observed for high mass diphoton resonances, with 2016 data, above the standard model predictions. Using leading order calculations from PYTHIA 8.2, RS gravitons with masses below 3.85 and 4.45 TeV are excluded for $k = 0.1$ and 0.2 respectively. For $k = 0.01$, graviton masses below 1.95 TeV are excluded, except for the region between 1.75 TeV and 1.85 TeV.

References
[1] CMS Collaboration [CMS Collaboration], "Search for resonant production of high mass photon pairs using $12.9\,\mathrm{fb}^{-1}$ of proton-proton collisions at $\sqrt{s} = 13$ TeV and combined interpretation of searches at 8 and 13 TeV," CMS-PAS-EXO-16-027.
[2] CMS Collaboration [CMS Collaboration], "Updated measurements of Higgs boson production in the diphoton decay channel at $\sqrt{s} = 13$ TeV in pp collisions at CMS.," CMS-PAS-HIG-16-020.
[3] CMS Collaboration [CMS Collaboration], "Measurements of properties of the Higgs boson and search for an additional resonance in the four-lepton final state at sqrt(s) = 13 TeV," CMS-PAS-HIG-16-033.
[4] G. Aad *et al.* [ATLAS Collaboration], "Observation of a new particle in the search for the Standard Model Higgs boson with the ATLAS detector at the LHC," Phys. Lett. B **716**, 1 (2012) doi:10.1016/j.physletb.2012.08.020 [arXiv:1207.7214 [hep-ex]].
[5] S. Chatrchyan *et al.* [CMS Collaboration], "Observation of a new boson at a mass of 125 GeV with the CMS experiment at the LHC," Phys. Lett. B **716**, 30 (2012) doi:10.1016/j.physletb.2012.08.021 [arXiv:1207.7235 [hep-ex]].
[6] V. Khachatryan *et al.* [CMS Collaboration], "Precise determination of the mass of the Higgs boson and tests of compatibility of its couplings with the standard model predictions using proton collisions at 7 and 8 TeV," Eur. Phys. J. C **75**, no. 5, 212 (2015) doi:10.1140/epjc/s10052-015-3351-7 [arXiv:1412.8662 [hep-ex]].
[7] G. Aad *et al.* [ATLAS Collaboration], "Measurements of the Higgs boson production and decay rates and coupling strengths using pp collision data at $\sqrt{s} = 7$ and 8 TeV in the ATLAS experiment," Eur. Phys. J. C **76**, no. 1, 6 (2016) doi:10.1140/epjc/s10052-015-3769-y [arXiv:1507.04548 [hep-ex]].
[8] G. Aad *et al.* [ATLAS and CMS Collaborations], "Combined Measurement of the Higgs Boson Mass in *pp* Collisions at $\sqrt{s} = 7$ and 8 TeV with the ATLAS and CMS Experiments," Phys. Rev. Lett. **114**, 191803 (2015) doi:10.1103/PhysRevLett.114.191803 [arXiv:1503.07589 [hep-ex]].
[9] V. Khachatryan *et al.* [CMS Collaboration], "Observation of the diphoton decay of the Higgs boson and measurement of its properties," Eur. Phys. J. C **74**, no. 10, 3076 (2014) doi:10.1140/epjc/s10052-014-3076-z [arXiv:1407.0558 [hep-ex]].
[10] CMS Collaboration [CMS Collaboration], "Studies of Higgs boson production in the four-lepton final state at $\sqrt{s} = 13$ TeV," CMS-PAS-HIG-15-004.
[11] V. Khachatryan *et al.* [CMS Collaboration], "Search for Resonant Production of High-Mass Photon Pairs in Proton-Proton Collisions at $\sqrt{s}$ =8 and 13 TeV," Phys. Rev. Lett. **117**, no. 5, 051802 (2016) doi:10.1103/PhysRevLett.117.051802 [arXiv:1606.04093 [hep-ex]].
[12] S. Chatrchyan *et al.* [CMS Collaboration], "The CMS experiment at the CERN LHC," JINST **3**, S08004 (2008). doi:10.1088/1748-0221/3/08/S08004
[13] CMS Collaboration [CMS Collaboration], "Particle-Flow Event Reconstruction in CMS and Performance for Jets, Taus, and MET," CMS-PAS-PFT-09-001
[14] "Commissioning of the particle-flow event with the first LHC collisions recorded in the CMS detector," CMS-PAS-PFT-10-001
[15] T. Sjstrand *et al.*, "An Introduction to PYTHIA 8.2," Comput. Phys. Commun. **191**, 159 (2015) doi:10.1016/j.cpc.2015.01.024 [arXiv:1410.3012 [hep-ph]].
[16] J. Allison *et al.*, "Geant4 developments and applications," IEEE Trans. Nucl. Sci. **53**, 270 (2006). doi:10.1109/TNS.2006.869826
[17] P. D. Dauncey, M. Kenzie, N. Wardle and G. J. Davies, "Handling uncertainties in background shapes : the discrete profiling method," JINST **10**, no. 04, P04015 (2015) doi:10.1088/1748-0221/10/04/P04015 [arXiv:1408.6865 [physics.data-an]].
[18] G. Aad *et al.* [ATLAS and CMS Collaborations], "Combined Measurement of the Higgs Boson Mass in *pp*

Collisions at $\sqrt{s} = 7$ and 8 TeV with the ATLAS and CMS Experiments," Phys. Rev. Lett. **114**, 191803 (2015) doi:10.1103/PhysRevLett.114.191803 [arXiv:1503.07589 [hep-ex]].